Chapter 4

Grain Boundary in Oxide Scale During High-Temperature Metal Processing

Xianglong Yu and Ji Zhou

Additional information is available at the end of the chapter

http://dx.doi.org/10.5772/66211

Abstract

Grain boundary in oxide scale has profound influences on the deformation behaviour and tribological properties of metal alloys at high temperature. This chapter introduces some recent progress to quantify microstructure and interface quality, providing examples of possible property variations. Some fundamental issues of oxidation mechanism have been given, consisting of crystal structures of iron oxides and oxidation of steel alloys. Two main things are addressed: One is what the characters of grain boundaries are developed in the oxide scale, which is associated with grain shape and size, microtexture, and special grain boundaries such as coincident site lattice (CSL) boundaries. Another is the role of grain boundaries played during metal processing, including initial oxidation via grain boundary diffusion, stress and deformation processing, and tribological properties of oxide scale at metal processing. Finally, a more extensive effort was also made to summarise the experimental techniques used to investigate oxide scale.

Keywords: grain boundary, oxide scale, oxidation, steel, metal processing

1. Introduction

Metallic oxides are inevitable to generate on the surface of steel products during metal forming processes at high temperature. If its thickness is larger than nanometre size, the oxide layer can be termed as *oxide scale* in industrial manufacturing. The formation of oxide scale or the oxidation of industrial materials depends, not only on the properties of their component crystals, but also on those of the boundaries between those crystals, in particular the structure and chemical composition of the boundaries.

Grain boundaries have distinct properties relative to bulk material in terms of atomic coordination, reactivity and diffusion rates. Phase contact creates interfaces that represent changes

in composition with disrupted atomic bonding. Grain boundary refers to the interface zone between grains of the same phase, while interfaces are boundaries between dissimilar phases. It represents the narrow zone where atomic bonding is disrupted by misalignment of the crystalline grains. This disrupted bonding at the grain boundary is about 5–10 atoms across. Grain boundaries have nanoscale spatial dimensions, which can generate substantial resistance to ionic transport due to dopant (or impurity) segregation. This diffusion provides active paths for atomic motion, particularly at high temperature, during the diffusion-controlled oxidation or corrosion. Thus, composite properties are sensitive to the interface structure and chemistry to large potential variations.

This crystallographic structure of a metal alloy is one of the important parameters in determining the oxidation or corrosion behaviour. The characters of grain boundaries in oxide layers formed on substrates influence adhesion and friction behaviour, surface fracture and wear during high temperature steel processing. However, the effect of grain characters on the oxidation behaviour is not fully understood yet. There are still many challenges, one of which is how to engineer grain boundaries to optimise the oxidation resistance of these materials. For this reason, detailed understanding of the processing-structure-property relationships that focus on grain boundaries and interfaces is critical to advanced manufacturing of metals. Furthermore, it is necessary to modify the grain boundary characteristics of this alloy which affect its oxidation resistance.

In this chapter, an attempt has been made to explore the role and behaviour of grain boundaries in the oxide scale formed on the steel surface during metal processing. In doing so, two things we need to consider for such high-temperature plastic deformation are diffusion mechanism at grain boundaries and resulting boundary migration in the growth of grains.

2. High-temperature oxidation

This section is devoted to the fundamental issues of oxidation mechanism that should be defined and summarised before specific problems are confronted. During metal processing at elevated temperatures, oxidation occurs inevitably on the surface of products. In the case of the pure iron, the oxide scale formed on is a complex mixture of three iron oxide phases: hematite (Fe_2O_3), magnetite (Fe_3O_4) and wustite ($Fe_{1-x}O$, x = 0.84–0.95) [1]. This is because iron has divalent and trivalent ions (Fe^{2+} and Fe^{3+}). The complete oxidation of iron can be divided into three main steps, where iron oxidises to the lowest valence ion Fe^{2+} and forms the first sub-layer of wustite ($Fe_{1-x}O$) next to the metal. Then, some of Fe^{2+} ions oxidise further to Fe^{3+} and contain both valence iron ions as the intermediate sub-layer of magnetite (Fe_3O_4). Under conditions of sufficient oxygen, the outer sub-layer of hematite (Fe_2O_3) only consists of the highest valence iron ion Fe^{3+}. This is the case above 570°C (the eutectoid point of the Fe-O system) in the diffusion-controlled growth of multilayered scales on pure iron. Below 570°C, the wustite phase is unstable, and the oxidation of iron directly results in magnetite. In steel, various Fe-C alloys, their oxidation at high temperature can be more complex than pure iron, in particular the segregation of different element at grain boundaries.

http://dx.doi.org/10.5772/66211

2.1. Iron oxides

In view of the iron cations can exist in the two valence states, iron oxides can have different crystal structures with different Fe/O ratios. These phases include wustite ($Fe_{1-x}O$), magnetite (Fe_3O_4) and hematite (α-Fe_2O_3) [2].

Wustite has a defective halite structure, with anion sites occupied by O^{2-} and most cation sites occupied by divalent Fe^{2+} ions. Cubic close-packed (CCP) array of O^{2-} stacked along the [111] direction. Most of the iron is octahedral with a small proportion of Fe^{3+} on the vacant tetrahedral sites (**Figure 1a**). A cation-deficient phase written as $Fe_{1-x}O$ (with 1_x ranging from 0.83 to 0.95) exists at 0.1 MPa pressure and temperatures higher than 570°C. Wustite is a p-type (p = positive carrier) semi-conducting oxide with a high concentration of lattice defects. These high cation vacancies result in a high mobility of cations and electron via metal vacancies and electron holes.

Magnetite (Fe_3O_4) has an inverse spinel structure containing both divalent and trivalent iron ions. The distribution of its cation is written as (Fe^{3+}) [$Fe^{3+}Fe^{2+}$] O_4, where the parentheses denote the tetrahedral sites and the square brackets denote the octahedral sites. In this case, the ferric ion Fe^{3+} relinquishes half of the octahedral sites to the ferrous species Fe^{2+}, that is, with $8Fe^{3+}$ ions located in tetrahedral sites plus ($8Fe^{3+}$ and $8Fe^{2+}$) ions distributed into octahedral sites per unit cell. The structure consists of octahedral and mixed tetrahedral/octahedral layers stacked along the [111] direction. **Figure 1b** shows the sequence of Fe- and O-layers and the section of this structure with three octahedral and two tetrahedral. Magnetite with an excess of oxygen also exists, but this excess is much smaller than that with wustite, and the corresponding concentration of defects is also less.

The crystal system of hematite (α-Fe_2O_3) is a rhombohedral structure (**Figure 1c**) with a low concentration of structural defects. Hexagonal close-packed (HCP) arrays of oxygen ions are stacked at the [001] direction. The O-O distances along the shared face of an octahedron are shorter (0.2669 nm) than the distance along the unshared edge (0.3035 nm), and hence, the octahedron is distorted trigonally. The shared Fe-O_3-Fe triplet structure influences the

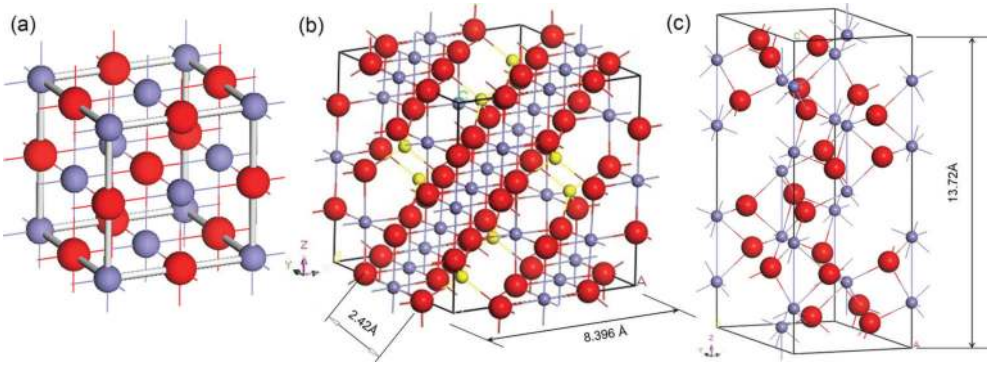

Figure 1. Crystal structure of (a) wustite (FeO), (b) magnetite (Fe_3O_4) and (c) hematite (α-Fe_2O_3).

magnetic properties of the oxide because hematite is an n-type (n = negative carrier) semiconducting oxide in which the diffusion of anions is dominant.

In a word, these iron oxides have the different crystal symmetries representing by a different space group: ferrite, *Im-3m*; wustite, *Fm-3m*; magnetite, *Fd-3m*; hematite, *R-3c*, and different lattice parameters: ferrite, wustite and magnetite in cubic symmetry with lattice parameters (a) of 0.287, 0.431 and 0.840 nm, respectively, and hematite in a trigonal structure with a = 0.504 nm and b = 1.377 nm [3].

2.2. Oxidation of steel alloys

Due to the presence of alloying elements and impurities in Fe-C steel alloys, the oxidation rates, phase development and morphologies of oxide scale are dramatically different from pure iron under various processing parameters. The reader can be referred to some published books [1], with regard to these four factors, alloying elements, oxidation kinetics, resulting oxides and their microstructure. More attention will be given here to the relationships between theories associated with grain boundaries of oxide scale.

The oxide scale formed on low carbon steels generally consists of a typical three-layered microstructure with a thin outer layer of hematite (Fe_2O_3), an intermediate layer of magnetite (Fe_3O_4) and an inner layer of wustite ($Fe_{1-x}O$, 1_x = 0.84–0.95) adjacent to the steel substrate [4]. This three-layered microstructure remains until a eutectoid point of the Fe-O phase equilibrium diagram is reached if oxygen is available at a temperature of 570°C. When the temperature drops below 570°C, the wustite phase becomes unstable and will decompose into eutectoid products of magnetite and ferrite. During the cooling from high temperature, the morphology and composition within oxide scale will be changed significantly. This variation mainly depends on heat treatments, atmosphere of the gas and chemistry of steels.

Analogous to the alloying strength in steel substrate, the alloying additions modified the oxidation quite dramatically. Normally, the amount of silicon and chromium aims to form a protective oxide scale, whereas small additions of nickel, copper, niobium, molybdenum and vanadium led to a greatly increased adherence of oxide scale. For instance, silicon generally enriches and forms an anchor-like morphology at the oxide scale/steel interface or grain boundaries of the oxides. Manganese is normally used as a solvent, while the transport of carbon is via defects such as pores rather than lattice or grain boundary diffusion. Because manganese has a stronger affinity for oxygen than iron does, manganese is normally spread sparingly over the entire oxide layer in the cross-sectional direction [3]. In addition to alloying elements, the atmosphere of gas as it interacted with oxides, especially water vapour, has made our understanding of the overall situation elusive [5], while the different behaviour of steel alloys in air-moisture mixtures has further complicated the set of observations.

The thickness or weight change in oxide scale with time is generally used to assess oxidation rates of the metallic alloys. In a linear or parabolic growth rate, the mixed para-linear kinetics is widely accepted to deal with the short-time growth of oxide scale during high-temperature metal processing. With the oxidation of steels below 727°C (the eutectoid point of the Fe-C system [4]), the oxidation kinetics is similar to pure iron due to without decarburisation at

http://dx.doi.org/10.5772/66211

various atmospheres and follows approximately parabolic kinetics. In a case of oxidation in pure iron at 700–1200°C, the thickness ratio between 100:5:1 and 100:10:1 ($FeO:Fe_3O_4:Fe_2O_3$) can be obtained, whereas at 400 and 550°C without wustite, it can be 10:1 to 20:1 ($Fe_3O_4:Fe_2O_3$) [6]. The phase development during the high-temperature oxidation of steel alloys concentrated mostly on the evolution of wustite during isothermal holding because wustite will decompose into magnetite and ferrite below 570°C.

The oxide scale consists of most magnetite and hematite at room temperature. Three research directions can be: wustite formation above 700°C, magnetite and hematite below 570°C and wustite decomposition between two temperature ranges. This chapter here only focuses the morphologies of oxide scale at room temperature cooling from high-temperature processing. It is noted that this scheme, using microstructures at room temperature to deduce what happened at high temperature, can thus far be subject to the current characterisation techniques. If one *in situ* technique is available to observe oxidation behaviour at high temperatures around 1000°C, especially during a long term, some current results could be improved significantly.

3. Characteristics of grain boundaries in oxide scale

This section covers the microstructure or morphologies, the crystallographic preferred orientation (i.e. texture) and characteristics of grain boundaries in the magnetite/hematite oxide scale.

3.1. Microstructure characterisation

Figure 2 shows the oxidised samples in the cross-sectional or thickness direction parallel to the direction of oxide growth and from the top surface. Electron backscattered diffraction (EBSD) phase mapping shown in **Figure 2a** and **b** indicates a columnar-shape microstructure between the outer granular grains and the globular inner layer [7]. The oxide scale is composed of a thin outer layer of hematite and the inner duplex magnetite layers. The outer layer is columnar in structure, whereas the inner layer is much finer grained and the grains are equiaxed. The grains of magnetite have granular shape with the grain size around 3 μm in the outer layer of oxide scale. In addition, hematite near the surface gradually penetrates into the cracks within the oxide scale.

Grain shape and size highly influence the oxidation of pure metals and their alloys at high temperature. Oxidised scale shows the rough microstructure with valleys around grain boundary (**Figure 2c**, **d** [8]). This indicates that the transport of cations along grain boundaries is the dominant mechanism for outer scale growth. The diffusion of metal ions can result in vacancies and cavity to facilitate the formation of local pores [8]. Therefore, the grain-refined metal substrate can enhance the grain boundary diffusion at high temperature.

3.2. Microtexture evolution of oxide scale

Crystallographic orientation refers to how the atomic planes in a volume of crystal or grain are positioned relative to a fixed reference [9]. These grains present the occurrence of certain

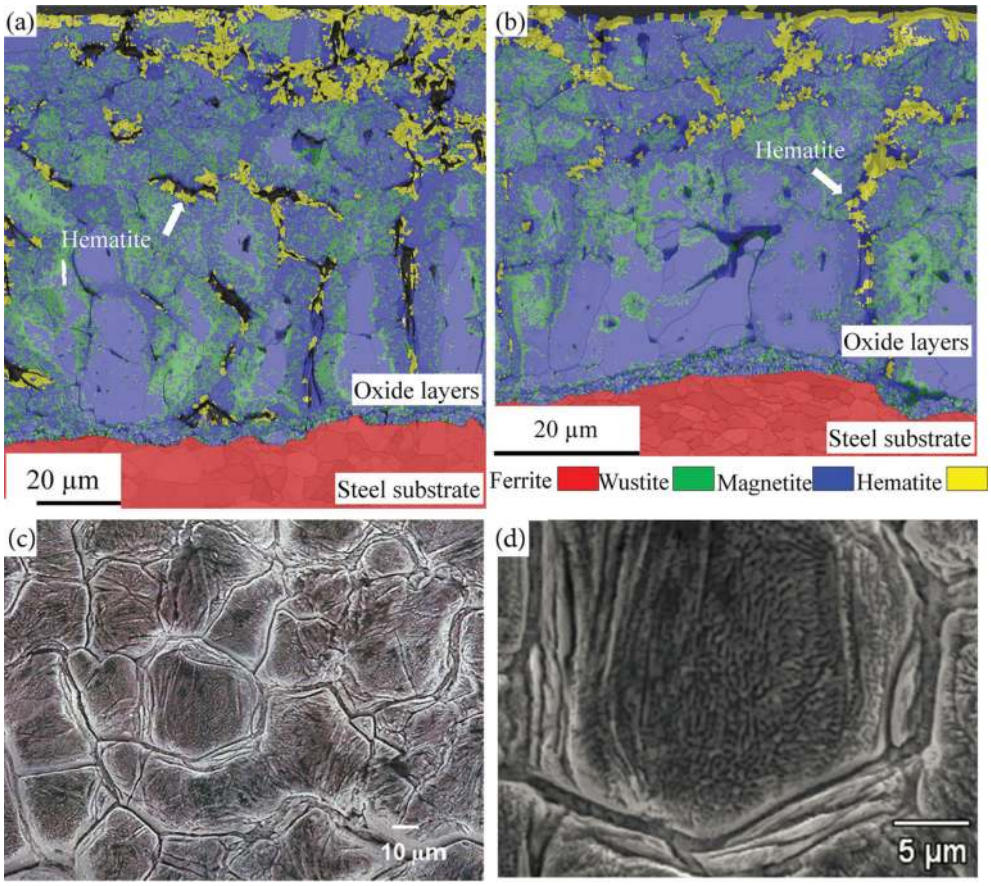

Figure 2. EBSD phase maps for wustite, hematite, magnetite and ferrite of the microalloyed steel hot rolled at 860°C with the thickness reductions and then cooling rates of (a) 10%, 10°C/s, and (b) 13%, 23°C/s [7], (c) SEM morphologies of top oxide scale formed over pure iron and (d) the magnification of one of valley surface [8].

orientations caused by heat treatments from melting and subsequently thermomechanical processing. This tendency is known as preferred orientation or texture. *Microtexture* is the conjoining of microstructure and texture [9], referring to the orientation statistics of a population of individual grains and their spatial location, that is, the orientation topography. To avoid ambiguity, a texture that reflects an average value obtained from many different grains is often called macrotexture [9]. Microtexture can generally be representing by pole figure, inverse pole figure or orientation distribution functions (ODF). Pole figure and inverse pole figure can be defined by the projection of orientation space through the crystal to specimen coordinate system or vice versa. ODF in the form of sections through the orientation space express the probability density function of orientations. This is a quantitative evaluation of the microtextures made by means of spherical harmonics method.

http://dx.doi.org/10.5772/66211

Analysis of the microtexture in the oxide phases and their orientation relationship is now being studied. A strong {001} texture may be found in wustite whatever the steel substrate [10], though this fibre texture also evolves in magnetite under low-temperature oxidation [6]. **Figure 3** shows texture development of magnetite and hematite in deformed oxide layers and their intensity distributions along associated fibres or texture components. Magnetite has a cubic structure, and its ODF sections are depicted using the ϕ_2 = 0° and 45° (**Figure 3b**) in terms of the Bunge system. In contrast, for hexagonal hematite, the ODF sections with ϕ_2 = 0° and 30° (**Figure 3d**) are used [9]. θ fibre develops in magnetite superimpose on ϕ_2 = 0° section at Φ = 0° with the rotations of <100>//ND [6, 11]. **Figure 3a** shows the intensity distribution of the θ fibre in magnetite on the samples subjected to various deformation conditions. <10-10> fibre component in α-Fe_2O_3 (**Figure 3c**) lies on ϕ_2 = 30° section and corresponds to orientations along Φ = 90°.

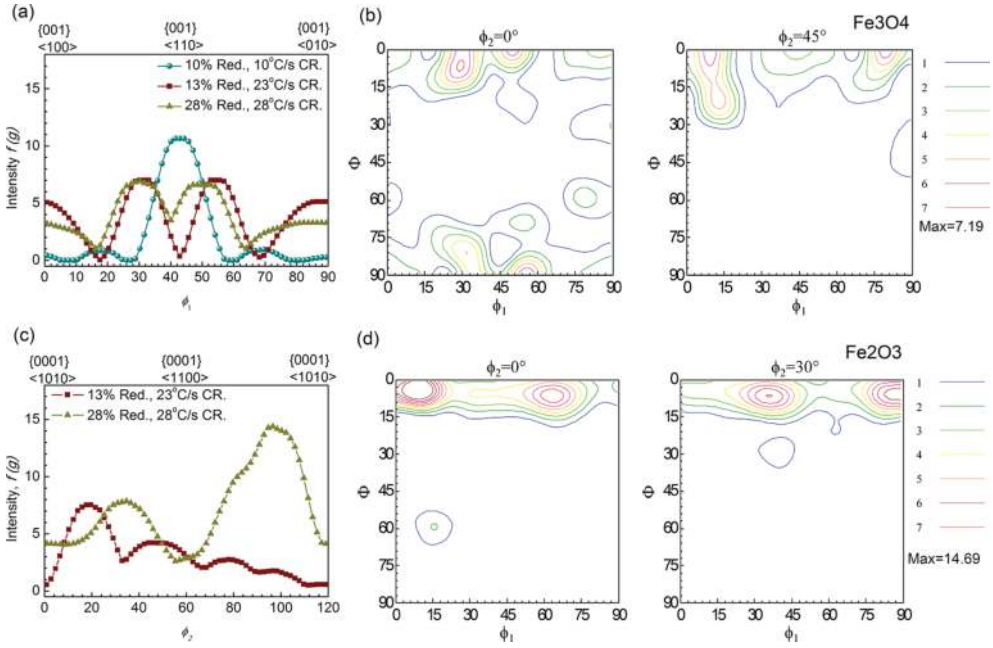

Figure 3. Development of texture intensity *f*(*g*) along the (a) θ fibre of magnetite, (c) <1010> fibre of hematite, of the samples with different thickness reductions (TRs) and cooling rates (CRs), and orientation distribution function (ODF) sections for (b) magnetite and (d) hematite at a TR of 28% and a CR of 28°C/s [12].

Study on orientation relationship of oxide phase is still less explored thus far. A cube-cube orientation relationship between wustite and magnetite may prevail in undeformed oxide scale possibly due to the defective structure of the wustite. The orientation of the magnetite and substrate was reported {110}Fe//{100}Fe_3O_4, <110>Fe//<100>Fe_3O_4 in the case of transforming by continuous cooling from 400°C. By contrast, the Fe/FeO orientation relationship was {100}

Fe//{110}FeO, <110>Fe//<110>FeO. For a very thin oxide scale, a Fe/FeO orientation relationship was {100}Fe//{100}FeO, <100>Fe//<110>FeO [13].

3.3. Character distribution of grain boundaries

Effects of grain orientation and grain boundary characters on the elevated temperature oxidation behaviour demonstrate the role of grain boundaries in enhancing high-temperature oxidation resistance of various polycrystalline steel alloys. Overall surface energy and tribological behaviour can also be enhanced by grain boundary engineering.

3.3.1. Grain boundaries

Grain boundaries can be classified geometrically in terms of the relative misorientation between the neighboured grains. This relative misorientation can be defined by misorientation axis and angle. For instance, $2° \leq \theta < 15°$ misorientations are defined as low-angle grain boundaries (LAGBs), whereas the high-angle grain boundaries (HAGBs) are ≥15°. Certain specific combinations resulting in a coincidence site lattice (CSL), the degree of coincidence is represented by the reciprocal density of common lattice points, denoted as the Σ number. As such, special grain boundaries refer to the low $\sum$ ($\sum \leq 29$) CSL boundaries, even though there is no physical basis for this assumption [14].

In oxidation and corrosion, it is widely believed that HAGBs have undergone hot corrosion and substantial depletion/segregation of alloying elements through the entire cross section. Distribution of grain boundaries in surface layer of oxide scale reveals that the misorientation tends to be large near grain boundaries, particularly at the oxide-substrate interface, where the high fraction of small magnetite grains is accumulated.

3.3.2. Special grain boundaries

Low-energy CSL boundaries with higher mobility can enhance the resistance of cracking or oxidation [15, 16]. CSL boundaries with low Σ orientation ($\Sigma \leq 49$) display improved physical and chemical properties relative to general or high CSL boundaries ($\Sigma > 49$) [17]. Some studies [18] reported that the resistance to intergranular oxidation of Ni-Fe alloy increased upon increasing the fraction of special boundaries. The extent of oxidation of individual Σ boundaries in Ni-Fe alloys is based on morphological observations. It found that Σ3, Σ11 and Σ19 were more resistant to oxidation than other Σ boundaries [19].

In a oxidised microalloyed low carbon steel [12], a high proportion of low-angle and low-ΣCSL boundaries, magnetite for 60°/<111> (Σ3), and hematite for 57.42°/<1-210> (Σ13b) and 84.78°/<0-110> (Σ19c) can be found. Misorientation peaks occur in α-Fe_2O_3 for axes near <0001> in the angle range of 27°–63° and <102> in the angle range of 63°–83°. For α-Fe_2O_3, the relatively high densities correspond to 57.42°/<110> (Σ13b) and 84.78°/<010> (Σ19c).

Furthermore, CSL boundaries distributions in **Figure 4** [17] reveal that Fe_3O_4 carries a high proportion of Σ3, Σ5 and Σ7, whereas α-Fe_2O_3 has a profound fraction of Σ7, Σ13b and Σ19c. It is noted that coherent twins have been excluded from this analysis, which results in a significantly lower fraction of Σ3 boundaries. In any case, it becomes clear that these low CSL grain

http://dx.doi.org/10.5772/66211

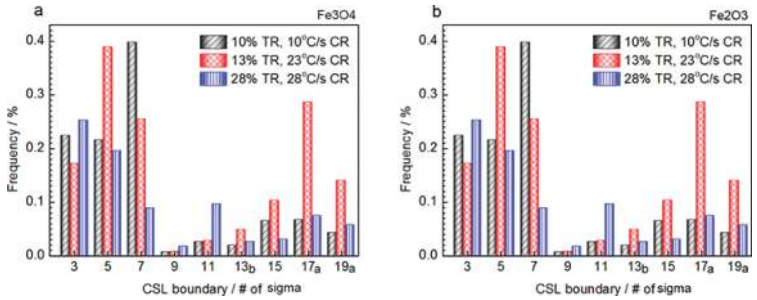

Figure 4. Histogram plots of CSL boundary distribution for (a) Fe_3O_4 and (b) α-Fe_2O_3, of the samples with different thickness reductions (TRs) and cooling rates (CRs) of oxide scale formed on a microalloyed low carbon steel [17].

boundary characteristics in Fe_3O_4 and α-Fe_2O_3 can be used to enhance crack resistance and further improve tribological properties of oxidised steels during high-temperature processing.

4. Roles of grain boundaries in oxide scale

The grain boundaries of either wustite, magnetite or hematite play a significant roles in the oxidation of metals and during their processing at high temperature. Three stages can be divided into: (i) diffusion-controlled oxidation of metal alloys; (ii) the plastic deformation mechanism near grain boundaries and resulting fracture of oxide scales; and (iii) tribological properties of oxide scale consisting various different grain boundaries during metal processing. All these above are this section will address.

4.1. Diffusion-controlled oxidation mechanism in grain boundaries

Grain characters, such as grain shape or grain boundary, highly influence the oxidation kinetics of pure metals and alloys. Grain boundary diffusion is more predominant in iron metal oxidation at high temperature. At low temperatures, the role of grain boundary diffusion as a main factor in comparison with other short circuits remains elusive.

To understand the role of grain boundary in diffusion-controlled oxidation, it is essential to detect which types of grain boundaries are involved. The EBSD/X-ray energy dispersive spectroscopy (EDS) map scanning can analyse the elemental distribution and correlate with the grain boundary character, and hence visualise the type of grain boundaries that are susceptible to hot corrosion or oxidation. **Figure 5** shows the image quality plus grain boundary map of the cross section of the hot corrosion alloy 617 [14] and EDS elemental distribution maps of various alloying elements. Preferential segregation/depletion of alloying elements occurred at grain boundaries: the segregation of Mo, S, Co and Ni at the random HAGBs along with a depletion of Cr after hot corrosion. The presence of S segregations also at intact interfaces and at oxide grain boundaries affects the oxide growth mechanism [20]. $\sum 3$ boundaries show few preferential enrichment/depletion of any alloying element, that is, indicating that these boundaries are resistant to hot corrosion.

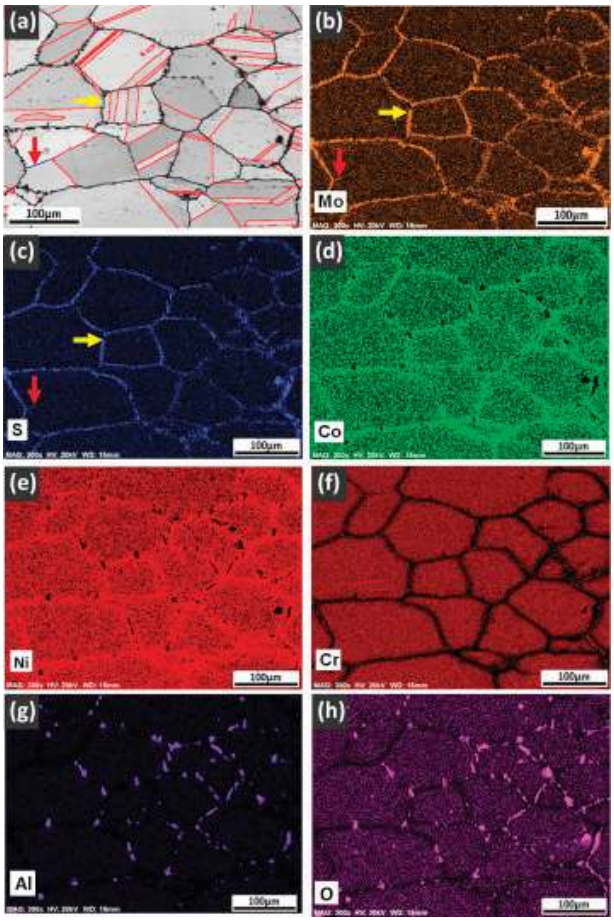

Figure 5. (a) Image quality plus grain boundary map (colour code: ∑3-red, ∑9-blue, ∑27-green, random HAGBs-black) and EDS elemental map showing distribution of (b) Mo, (c) S, (d) Co, (e) Ni, (f) Cr, (g) Al and (h) O across the cross section of the alloy 617 after hot corrosion testing [14].

Two dominant diffusion can occur at grain boundary or lattices [8]. Surface diffusion happens at lower temperatures compared to grain boundary diffusion, and volume diffusion is active only at very high temperatures. With a small grain size, the higher grain boundary area naturally increases grain boundary diffusion [21]. Grain boundary diffusion is more sensitive to grain size when compared to volume diffusion. In contrast to lattice diffusion, the control of elemental diffusion at the grain boundaries can be effective to have a thin and compact oxide scale on the Fe-Cr alloy surface [22]. This suggests that the grain boundary diffusion is confined at the initial of oxidation, while the oxide layer is relatively thin.

In a stainless steel of cyclic steam oxidation, the previous results [23] indicate that grain boundaries not only promote the chromium outward diffusion, but also provide the fast diffusion

http://dx.doi.org/10.5772/66211

paths for the oxygen penetration. The grain boundaries promote the iron outward diffusion, accompanied with the fast growth of interfacial voids between two oxide layers. In a Ni-5Cr alloy, intergranular selective oxidation also accompanied by local chromium depletion and diffusion-induced grain boundary migration. Recently, coupled transmission electron microscope (TEM)/APT surface and grain boundary oxide compositions were identified, and Ni enrichment was observed around the oxides. The data provide novel information on the role of the minor impurities and the formation of early-stage oxides in 304 stainless steel [24]. However, copper diffusion along grain boundaries is not the main mechanism in this case. A high-resolution characterisation of the oxide–metal interface has shown the presence of a Fe-rich oxide, less dense than the original Cr-rich oxide [25]. It is reasonable that the Gibbs free energy reduction with Cu spinel solid solution formation in hematite at high oxygen partial pressure induces the bulk diffusion of Cu through hematite grains to the top surface of external oxide [26].

Various diffusion mechanisms can differ from types of grain boundaries in different oxidised substrates, for example, CSL special grain boundaries in ferritic stainless steel [18], whereas high-angle grain boundaries in Al_2O_3 [27]. Diffusion-controlled oxidation mechanism of the oxides thermally grown on the metal surface is similar to the pure oxides in bulk ceramics, ranging from a point effect mechanism to migration of disconnections, grain boundary ledge defects [27].

4.2. Deformation mechanism near grain boundaries

This section will discuss the internal stress state after diffusion-controlled oxidation of metal alloys and plastic deformation of oxide scales during metal processing. The occurrence of concomitant grain boundary sliding in the thermally grown oxides may be evidenced leading then to the corresponding microscopic strain. Local strain caused by the oxidation of magnetite to hematite can cause inter crystalline microcracks. These microcrackings can induce plastic deformation under differential contraction and to open diffusion paths inducing grain boundary diffusion.

Cracking propagation can roughly attribute to alloying elements segregation at grain boundaries. To delve, then which types of grain boundaries will occur these elements accumulation, and which types of alloying elements would be detrimental to crack propagation? For example, the Co oxide enriches at the boundaries of high stacking fault (SF)/low SF grains [28] and the Ni/Ti/Al-rich oxides at normal grain boundaries. But the enrichments of these elements have slightly influence on crack initiation and propagation in some Ni-based superalloy.

The mechanical stresses in the oxide scale play a significant role in its integrity. Generally, internal stresses are induced by the growth of oxides, thermal expansion mismatch and applied forces [6], some of which originate from many different causes. The formation and propagation of cracks generally occur along grain boundaries of oxide scale. The stress is the greatest at the tips of small cracks in the material, and consequently, the reaction proceeds at its greatest rate from these tips. To alleviate the propagation of cracks, low-angle and low-ΣCSL boundaries in microstructure can offer obstacles, because they minimise the solute effects and reduce the interaction between the interfaces and glissile dislocation. In the case of

magnetite/hematite scale [17], the oxide scale is easy to crack in presence of Σ13b and Σ19c in α-Fe_2O_3 compared to Fe_3O_4 with Σ3. Thus, it is possible that during this time, tailoring specific grain boundaries can provide new insight into means of suppressing propagation of cracks when it is undesirable and into means of producing specific trapped nanoparticles when it is desired.

One thing we should consider is to distinguish grain boundary strengthening to steel substrate or to formed oxide scale itself. Extensive studies have been focused on the role of grain boundaries played in the steel substrate. For instance, grain boundary strengthening and precipitation hardening are considered to provide the most to the high-strength properties of the mechanically alloyed oxide dispersion strengthened (ODS) ferritic alloys, containing nanosized (<3.5 nm) oxide dispersions. A higher density of these oxide particles with larger sizes than the ones in the matrix was found at the grain boundaries in ODS Fe–12Cr–5Al alloys (Y2O3 + ZrO2) (**Figure 6** [29]).

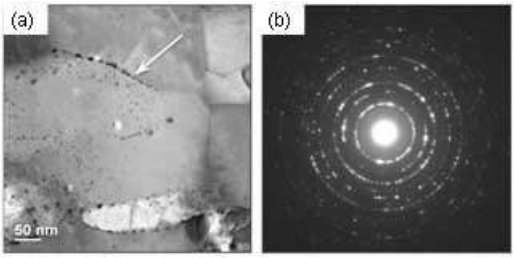

Figure 6. (a) High-angle annular dark field (HAADF)—scanning transmission electron microscopy (STEM) images of Fe–12Cr–5Al alloys (Y_2O_3 + ZrO_2) and (b) diffraction patterns after being mechanically alloyed and extruded at 950°C [29].

The grain refinement can be used to explain this strengthening process. Whatever grain boundaries works, the essential mechanism should be similar. However, the difference of a protective oxide scale containing reactive element may not simply be due to a site blocking effect in the grain boundary [30]. The contributions of dopant ions to the multiple electrical and ionic processes would provide valuable guidance to elucidate the deformation mechanism of oxide scale thermally formed on steel alloys. That is reason to note the difference between them as the presence of oxide particles at the grain boundaries and the temperature at which they were formed.

4.3. Effect of grain boundaries on tribological performance

Many different surface properties of metals and alloys will influence tribological performance. These surface properties include surface energy, crystallographic orientation, grain boundaries, texturing of surface and crystal structure. Grain boundaries in the oxide layers can alter the underlying failure mechanisms of formed oxide scale, which affects their tribological performance during metal processing. There are various strained conditions along grain boundaries because many dislocations present to help accommodate the misfit or mismatch

http://dx.doi.org/10.5772/66211

in adjacent orientations. These high energy regions at the surface could make sliding more difficult and increase the friction force of materials during metal forming.

Various mechanisms can be used to explain the role of grain boundaries in the tribolgoical properties of oxide scale during metal processing at high temperature. Our previous study [21] implies that grain boundary sliding contributes significantly to dissipation in oxide layers during hot rolling. If the oxidised grain boundary is under tension, both the metal and the oxide scale during thermal cycling tend to facilitate crack initiation [20]. A mechanism has been addressed for stress-aided grain boundary oxidation ahead of cracks. Oxygen embrittlement can therefore serve as the form of dynamic embrittlement or oxidation-induced grain boundary cracking during services at elevated temperatures [31]. In essence, the role of anisotropy needs to be investigated to clarify, which anisotropy (grain boundary energy or mobility) is dominant at which conditions. The local grain boundary planes can be dominated by the growing side of the boundary.

The friction characteristics with oxide scale also reveal a grain boundary effect—a profound dependence of friction on crystallographic direction and orientation and grain boundary characters. The variation of the coefficient of friction and rolling force in different thickness reductions during hot rolling associated with microtexture and grain boundary characters in magnetite/hematite scale formed on a microalloyed low carbon steel [17].

In summary, the role of grain boundary chemistry and structure on fundamental mechanisms and properties of oxide scale can help to accelerate the design optimisation of grain boundaries in oxidation or corrosion resistance.

5. Methodological potentials

Before starting, we need to consider some sample preparations to detect grain boundaries. Two directions are generally used to observe the oxide scale formed on the metal surface. One is the cross-sectional or thickness direction of the oxidised sample, parallel to the direction of oxide growth. Another is the top surface of oxidised sample suitable for the relatively thin oxide layers or the initial oxidation conditions. In order to visualise the grain boundary, the testing sample can be polished using mechanical and chemical-mechanical polishing methods. Particularly, it is necessary to select different etchants for different compositions in the oxide scale or metal substrate. Sometimes, this classical polishing/etching method cannot observe the grain morphologies both the oxide scale and the substrate concurrently. In electron backscattered diffraction (EBSD) technique and transmission electron microscope (TEM), the grain characters can be detected clearly without etching the sample. EBSD can use normal ion milling to prepare the sample. This is can make easier than TEM because TEM need to reduce the thickness of the sample using focus ion milling beam (FIB) or other advanced approaches. In a word, EBSD or TEM is generally used to observe the sample in cross-sectional direction, whereas scanning electron microscopy (SEM) can be used for top surface morphologies of oxidised sample. *In situ* electron microscopy cases are all the same but more challenging for the oxidation investigation.

Experimentally resolving and characterising grain boundary structure often requires a host of techniques: X-ray diffraction (XRD), scanning electron microscopy (SEM), electron backscattered diffraction (EBSD), transmission electron microscopy (TEM), X-ray energy dispersive spectroscopy (EDS) and electron energy loss spectroscopy (EELS). XRD or neutron diffraction normally deals with a texture that reflects an average value obtained from many different grains, that is, macrotexture. This chapter will address some techniques to obtain microtexture involving some individual grains.

5.1. Secondary electron microscope

Most grain boundary characters can be observed in low-vacuum secondary electron microscope (LV-SEM). In the backscattered electrons (BSE) mode, Z-contrast can assist phase identification. SEM/BSE hardly observe oxide scale and steel substrate without etching, because two parts of oxides and steel hardly to etching both using the same etchant. That is because polishing and etching for sample preparation can bring out the grain boundaries to more easily delineate individual grains. SEM/EDS and scanning transmission electron microscopy (STEM)/EELS help analyse the chemical species present and, combined with elemental mapping, can provide a distribution of the different chemistries in a spot, line or area. Sometimes, SEM can couple focus ion beam (FIB) to observe the grain characters along the cutting surface when preparing for TEM samples.

5.2. Electron backscattered diffraction EBSD

Electron backscattered diffraction (EBSD) can perform microstructure, phase identification, the crystallographic texture, and internal stresses, of oxidised sample. Some system can provide a transmission kikuchi diffraction (TKD) mode where the short working distance in backscattered electrons (BSE) detector as a complement. Various professional software suite fully integrated with image collection, versatile EBSD analysis and phase identification, can be used to acquire the online texture information and to analyse the offline scanning maps. Grain boundary mapping shows the crystallographic orientation of individual grains and the microstructure in the oxide scale [9]. Further, grain reconstruction can be carried out to delve the various mechanism associated with individual grains.

5.3. Transmission electron microscope

High-resolution transmission electron microscopy (HR-TEM) has improved microscopy resolution, more developed techniques, and coupling with advanced approaches will enable the understanding and engineering of grain boundaries (including twins) and intergranular films. For instance, scanning transmission electron microscopy (STEM) coupled with electron energy loss spectroscopy (EELS) is capable of simultaneously mapping the atomic/electronic structure of light elements such as oxygen at adequate spatial resolution. The electronic state of the elements across the boundary can be identified by STEM-EELS line scan crossing the grain boundary in steps of a few nanometres [32]. TEM imaging further resolves details of the crystal structure of grains and grain boundaries.

http://dx.doi.org/10.5772/66211

5.4. More advanced techniques

Atom probe tomography has some unique virtues for hydrogen detection, such as near-atomic resolution and equal sensitivity to all elements in the periodic table. The advanced technique has been used to investigate hydrogen embrittlement in the oxide scale of two common zirconium alloys [33]. Grain boundaries of oxides can be low-field areas of the APT specimen and then can readily be identified [34]. A combined use of TEM and APT can be used to quantify grain boundary segregation and has been applied to the case of carbon GB segregation in ferrite [24] and intergranular oxidation of a Ni–4Al alloy [35].

For some corrosion environment, electrochemical scanning tunnelling microscopy (ECSTM) has applied to analyse *in situ* the passivation of grain boundaries on microcrystalline copper in 0.1 M NaOH aqueous solution [36]. ECSTM has provided accurate *in situ* topographic information on grain and grain boundary effects on the local active dissolution of microcrystalline copper in acid solution.

Time-of-flight secondary ion mass spectrometry (TOF-SIMS) provides elemental, chemical state and molecular information from surfaces of solid materials. Analogous to SEM/EDS instruments, TOF-SIMS aims to the compositional analysis of ultra-thin layers and nanoscale sample features. The difference is that TOF-SIMS can be used to characterise molecular information from organic materials and tissue sections for medical research.

6. Conclusions and future directions

This chapter covers the recent advance associated with grain boundaries in the oxide scale formed on metal alloys during metal processing. A number of benefits include (i) characterisation of grain boundaries ranging from microstructure, preferred orientations and different types of grain boundaries; (ii) the role of grain boundaries in the oxide scale playing in diffusion-controlled oxidation, deformation mechanism and tribological performance; and (iii) introducing the experimental techniques and analytical methodology underpinning this subject.

Some specific results can be concluded ranging from micotexture and grain boundaries characters. The (100) plane of magnetite is much more sensitive to the oxidation. In the coincident site lattice (CSL) boundaries, the $\sum 3$ in magnetite and $\sum 13b$ in hematite are dominant in the oxide scale. These findings suggest that low-angle grain boundaries and low-energy CSL boundaries can be used to prevent the initiation and propagation of cracks, further to enhance oxidation resistance of the materials.

Three current challenges dominate in the characterisation, mechanism and techniques for investigation the grain characters in oxide scale during metal processing at high temperature. First, grain characters consisting of grain shape and size, phase grain boundaries within oxide scale and orientation relationship between oxides are also need to be considered. Second, to delve which types of (special) grain boundaries to enhance the oxidation/corrosion resistance

and then to tailoring them. Finally, a combination of the various advanced techniques provides the frameworks for future investigation on the oxidation of the other metal alloys even bulk ceramics.

Acknowledgements

This work was supported by the China Postdoctoral Science Foundation under Grant No. 2015M580094, and the National Natural Science Foundation of China under Grant Nos.11274198 and 51532004.

Author details

Xianglong Yu* and Ji Zhou

*Address all correspondence to: xly991@uow.edu.au

State Key Laboratory of New Ceramics and Fine Processing, School of Materials Science and Engineering, Tsinghua University, China

References

[1] Birks N, Meier GH. Introduction of High Temperature Oxidation of Metals. 2nd ed. London: Cambridge University Press; 2006.

[2] Comel RM, Schwertmann U. The Iron Oxides: Structure, Properties, Reactions, Occurrence and Uses. New York: Wiley; 2003.

[3] Yu X, Jiang Z, Zhao J, Wei D, Zhou C, Huang Q. Microstructure and microtexture evolutions of deformed oxide layers on a hot-rolled microalloyed steel. Corrosion Science. 2015;**90**:140–152. doi:10.1016/j.corsci.2014.10.005

[4] Chen RY, Yuen WYD. Review of the high-temperature oxidation of iron and carbon steels in air or oxygen. Oxidation of Metals. 2003;**59**:433–468. doi:10.1023/A:1023685905159

[5] Saunders SRJ, Monteiro M, Rizzo F. The oxidation behaviour of metals and alloys at high temperatures in atmospheres containing water vapour: a review. Progress in Materials Science. 2008;**53**:775–837. doi:10.1016/j.pmatsci.2007.11.001

[6] Juricic C, Pinto H, Cardinali D, Klaus M, Genzel C, Pyzalla AR. Effect of substrate grain size on the growth, texture and internal stresses of iron oxide scales forming at 450°C. Oxidation of Metals. 2010;**73**:15–41. doi:10.1007/s11085-009-9162-1

[7] Yu X, Jiang Z, Zhao J, Wei D, Zhou C, Huang Q. Effect of a grain-refined microalloyed steel substrate on the formation mechanism of a tight oxide scale. Corrosion Science. 2014;**85**:115–125. doi:10.1016/j.corsci.2014.04.006

[8] Samal S, Mitra SK. Influence of grain shape, size, and grain boundary diffusion on high-temperature oxidation of pure metal Fe, Cu, and Zn. Metallurgical and Materials Transactions A. 2015;**46**:3324–3332. doi:10.1007/s11661-015-2987-0

[9] Engler O, Randle V. Introduction to Texture Analysis: Macrotexture, Microtexture and Orientation Mapping. 2nd ed. Boca Raton: CRC Press; 2010.

[10] Higginson RL, Roebuck B, Palmiere EJ. Texture development in oxide scales on steel substrates. Scripta Materialia. 2002;**47**:337–342. doi:10.1016/S1359-6462(02)00154-9

[11] Suárez L, Rodríguez-Calvillo P, Houbaert Y, Garza-Montes-de-Oca NF, Colás R. Analysis of deformed oxide layers grown on steel. Oxidation of Metals. 2011;**75**:281–295. doi:10.1007/s11085-010-9231-5

[12] Yu X, Jiang Z, Zhao J, Wei D, Zhou C, Huang Q. Crystallographic texture based analysis of Fe_3O_4/α-Fe_2O_3 scale formed on a hot-rolled microalloyed steel. ISIJ International. 2015;**55**:278–284. doi:10.2355/isijinternational.55.278

[13] Chang L, Lin SN. Analytical electron microscopy study of interfacial oxides formed on a hot-rolled low-carbon steel. Oxidation of Metals. 2005;**63**:131–144. doi:10.1007/s11085-004-3196-1

[14] Deepak K, Mandal S, Athreya CN, Kim D, de Boer B, Sarma S. Implication of grain boundary engineering on high temperature hot corrosion of alloy 617. Corrosion Science. 2016;**106**:293–297. doi:10.1016/j.corsci.2016.01.019

[15] Palumbo G, Aust KT, Lehockey EM, Erb U, Lin P. On a more restrictive geometric criterion for special CSL grain boundaries. Scripta Materialia. 1998;**38**:1685–1690. doi:10.1016/S1359-6462(98)00077-3

[16] Lehockey EM, Brennenstuhl AM, Thompson I. On the relationship between grain boundary connectivity, coincident site lattice boundaries, and intergranular stress corrosion cracking. Corrosion Science. 2004;**46**:2383–2404. doi:10.1016/j.corsci.2004.01.019

[17] Yu X, Jiang Z, Zhao J, Wei D, Zhou C, Huang Q. Effects of grain boundaries in oxide scale on tribological properties of nanoparticles lubrication. Wear. 2015;**332–333**:1286–1292. doi:10.1016/j.wear.2015.01.034

[18] Phaniraj MP, Kim DI, Cho YW. Effect of grain boundary characteristics on the oxidation behavior of ferritic stainless steel. Corrosion Science. 2011;**53**:4124–4130. doi:10.1016/j.corsci.2011.08.020

[19] Yamaura S, Igarashi Y, Tsurekawa S, Watanabe T. Structure-dependent intergranular oxidation in Ni–Fe polycrystalline alloy. Acta Materialia. 1999;**47**:1163–1174. doi:10.1016/S1359-6454(99)00007-5

[20] Fedorova E, Braccini M, Parry V, Pascal C, Mantel M, Roussel-Dherbey F, Oquab D, Wouters Y, Monceau D. Comparison of damaging behavior of oxide scales grown on austenitic stainless steels using tensile test and cyclic thermogravimetry. Corrosion Science. 2016;**103**:145–156. doi:10.1016/j.corsci.2015.11.012

[21] Yu X, Jiang Z, Zhao J, Wei D, Zhou J, Zhou C, Huang Q. Dependence of texture development on the grain size of tertiary oxide scales formed on a microalloyed steel. Surface and Coatings Technology. 2015;**272**:39–49. doi:10.1016/j.surfcoat.2015.04.026

[22] Horita T, Kishimoto H, Yamaji K, Xiong Y, Sakai N, Brito ME, Yokokawa H. Effect of grain boundaries on the formation of oxide scale in Fe–Cr alloy for SOFCs. Solid State Ionics. 2008;**179**:1320–1324. doi:10.1016/j.ssi.2008.01.090

[23] Yan J, Gao Y, Gu Y, Sun F, Yang Z, Lu J, Yin H, Li Y. Role of grain boundaries on the cyclic steam oxidation behaviour of 18-8 austenitic stainless steel. Oxidation of Metals. 2016;**85**:409–424. doi:10.1007/s11085-015-9603-y

[24] Kruska K, Lozano-Perez S, Saxey DW, Terachi T, Yamada T, Smith GDW. Nanoscale characterisation of grain boundary oxidation in cold-worked stainless steels. Corrosion Science. 2012;**63**:225–233. doi:10.1016/j.corsci.2012.06.030

[25] Kim JH, Kim DI, Shim JH, Yi KW. Investigation into the high temperature oxidation of Cu-bearing austenitic stainless steel using simultaneous electron backscatter diffraction-energy dispersive spectroscopy analysis. Corrosion Science. 2013;**77**:397–402. doi:10.1016/j.corsci.2013.08.015

[26] Dugdale H, Armstrong DEJ, Tarleton E, Roberts SG, Lozano-Perez S. How oxidized grain boundaries fail? Acta Materialia. 2013;**61**:4707–4713. doi:10.1016/j.actamat.2013.05.012

[27] Heuer AH, Azar MZ. A disconnection mechanism of enhanced grain boundary diffusion in Al_2O_3. Scripta Materialia. 2015;**102**:15–18. doi:10.1016/j.scriptamat.2015.01.026

[28] Jiang R, Gao N, Reed PAS. Influence of orientation-dependent grain boundary oxidation on fatigue cracking behaviour in an advanced Ni-based superalloy. Journal of Materials Science. 2015;**50**:4379–4386. doi:10.1007/s10853-015-8992-2

[29] Unocic KA, Pint BA, Hoelzer DT. Advanced TEM characterization of oxide nanoparticles in ODS Fe–12Cr–5Al alloys. Journal of Materials Science. 2016;**51**:9190–9206. doi:10.1007/s10853-016-0111-5

[30] Rettberg LH, Laux B, He MY, Hovis D, Heuer AH, Pollock TM. Growth stresses in thermally grown oxides on nickel-based single-crystal alloys. Metallurgical and Materials Transactions A. 2016;**47**:1132–1142. doi:10.1007/s11661-015-3273-x

[31] Chan KS. A grain boundary fracture model for predicting dynamic embrittlement and oxidation-induced cracking in superalloys. Metallurgical and Materials Transactions A. 2015;**46**:2491–2505. doi:10.1007/s11661-015-2860-1

[32] Lin Y, Fang S, Su D, Brinkman KS, Chen F. Enhancing grain boundary ionic conductivity in mixed ionic-electronic conductors. Nature Communications. 2015;**6**:6824. doi:10.1038/ncomms7824

[33] Sundell G, Thuvander M, Yatim AK, Nordin H, Andrén HO. Direct observation of hydrogen and deuterium in oxide grain boundaries in corroded Zirconium alloys. Corrosion Science. 2015;**90**:1–4. doi:10.1016/j.corsci.2014.10.016

[34] Kim JH, Kim BK, Kim DI, Choi PP, Raabe D, Yi KW. The role of grain boundaries in the initial oxidation behavior of austenitic stainless steel containing alloyed Cu at 700°C for advanced thermal power plant applications. Corrosion Science. 2015;**96**:52–66. doi:10.1016/j.corsci.2015.03.014

[35] Schreiber DK, Olszta MJ, Bruemmer SM. Directly correlated transmission electron microscopy and atom probe tomography of grain boundary oxidation in a Ni–Al binary alloy exposed to high-temperature water. Scripta Materialia. 2013;**69**:509–512. doi:10.1016/j.scriptamat.2013.06.008

[36] Chen H, Maurice V, Klein LH, Lapeire L, Verbeken K, Terryn H, Marcus P. Grain boundary passivation studied by *in situ* scanning tunneling microscopy on microcrystalline copper. Journal of Solid State Electrochemistry. 2015;**19**:3501–3509. doi:10.1007/s10008-015-2787-x